Periodica Polytechnica
Transportation Engineering

47(4), pp. 283-289, 2019
https://doi.org/10.3311/PPtr.12101

RESEARCH ARTICLE

The Effect of Iron Content on Microstructure and Porosity of Secondary AlSi7Mg0.3 Cast Alloy

Denisa Závodská[1*], Eva Tillová[1], Ivana Švecová[1], Mária Chalupová[1], Lenka Kuchariková[1], Juraj Belan[1]

Received 18 June 2017; accepted 18 February 2018

Abstract

In the present study, microstructure and porosity of AlSi7Mg0.3 cast alloy including various amounts (0.123; 0.454 and 0.655 wt. %) of iron were investigated. The alloys were produced as secondary (scrap-based - recycled). Iron leads to the formation of complex intermetallic phases during solidification, and how these phases can adversely affect mechanical properties, especially ductility, and also lead to the formation of excessive shrinkage porosity defects in castings. In order to determine the effect of iron addition to AlSi7Mg0.3 alloy, optical and SEM microscopy with EDX were used for microstructural examinations. Image analysis was conducted in order to determine effect of the Fe content on phases and porosity. It was found that increasing Fe content from 0.123 to 0.655 wt. % has no effect on SDAS but the morphology of Al-Si eutectic became finer. From EDX examinations, different Fe-based intermetallic phases (β-Al_5FeSi and α-$Al_{15}(FeMg)_3Si_2$) were observed. It was also observed that as Fe content increased, α-$Al_{15}(FeMg)_3Si_2$ phases was transformed into Al_5FeSi and the size and the number of Al_5FeSi phases increases. The image analysis results revealed that porosity values were by increasing Fe content increased too. We can to predict, that with the increasing amount of Fe decreasing the mechanical properties (first of all) ductility (through long β-Al_5FeSi intermetallic and high porosity).

Keywords

Al-Si cast alloy, microstructure, porosity, effect of Fe

[1] Department of Materials Engineering,
Faculty of Mechanical Engineering,
University of Žilina,
Univerzitná 8215/1, 010 26 Žilina, Slovak Republic
[*] Corresponding author, e-mail: denisa.zavodska@fstroj.uniza.sk

1 Introduction

Automotive - chassis, bodies, engine blocks, radiators, hubcaps, and etc. driven by consumer needs and increasingly tight regulations, the automobile industry has made ample recourse to aluminium. A European car today contains on average 100 kg of aluminium, taking advantage of multiple properties of the materials: lightness (a 100 kg loss of weight reduces fuel consumption by 0.6 litres/100 km and greenhouse gases by 20 %), resistance (improved road-handling, absorption of kinetic energy, shorter braking distance) and recycling (95 % of the aluminium contained in autos is collected and recycled, and represents over 50 % of the vehicle's total end-of-life value). Aluminium coming from recycling can allow 95 % energy savings and 85 % less CO_2 emissions compared to primary aluminium production. Recycling - aluminium can be recycled indefinitely without losing any of its intrinsic qualities. This is a considerable advantage in modern metallurgical industry. For the past 20 years the proportion of metal consumed that is recycled has grown steadily and today stands at something like 30 % of primary metal production (European Aluminium Association; Schlesinger, 2014; Hurtalová et al., 2013).

The Fig. 1 shows the fraction of world aluminium production from primary and secondary (recycled) sources. About one-third of the aluminium produced in the world is now obtained from secondary sources and in some countries the percentage is much higher. The process used for recycling aluminium scrap is very much different from those used to produce primary metal but in many ways follow the same general sequence. This sequence begins with mining ore, followed by mineral processing and thermal pre-treatment and then a melting step. The metal is then refined, cast into ingots and sent to customers. Aluminium alloys recyclers also face similar challenges to the producers of primary aluminium; there is need to produce a consistent alloy with the required chemistry, reduce the amount of waste generated, minimize energy usage and manufacture the highest-quality product at the lowest possible cost from raw materials of uncertain chemistry and condition (Mc Millan et al., 2012; Schlesinger, 2014).

Commercial Al-alloys always contain Fe, often as undesirable impurity and occasionally as a useful minor alloying

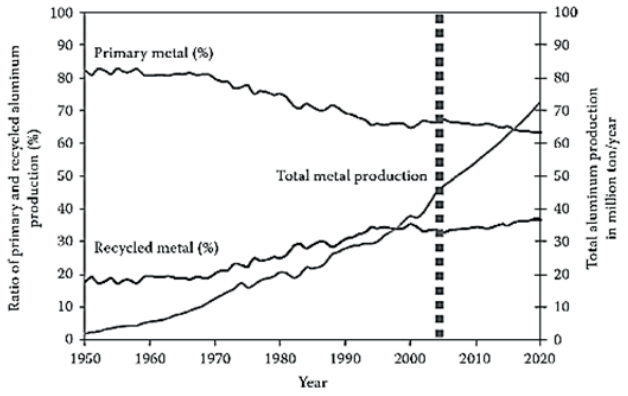

Fig. 1 Aluminium production and percentage from primary and secondary sources (Schlesinger, 2014).

element. As a minor alloying element, Fe has been used occasionally in Al-Cu-Ni alloys to enhance high temperature mechanical properties, in Al-Mg alloys to reduce coarsening, in Al-Fe-Ni alloys to enhance corrosion resistance in steam, and in high pressure die-cast (HPDC) Al-alloys to facilitate ejection and to help die-release (Schlesinger, 2014).

Iron is a natural impurity that arises during the manufacture of primary aluminium via the Bayer Process that converts bauxite (the ore) into alumina (the feedstock) and the subsequent Hall-Héroult electrolytic reduction process that converts alumina into molten aluminium (> 950 ºC). Depending on the quality of the incoming ore and the control of the various processing parameters and other raw materials, molten primary aluminium metal typically contains between 0.02 - 0.15 wt. % iron, with ~ 0.07 - 0.10 % being average (Schlesinger, 2014; Kuchariková et. al., 2016).

Secondary Al-alloys (produced from Al-scrap) contains higher background iron levels than the primary metal. Liquid aluminium can dissolve iron not only from the scraps, which have a higher Fe content than the primary metal, but also from unprotected steel tools and furnace equipment. Secondary alloys, particularly those destined for high-pressure die casting process, can contain iron levels up to 1.5 % (Ceschini et al., 2009).

In an amount 0.3 - 0.5 wt. % of Fe, it prevents sticking casting on the metal mould, increases the strength and in larger quantities also the heat resistant. At higher contents, as 0.3 - 0.5 wt. % of Fe, it causes first of all formation of Fe-intermetallic phases (e.g. Al_5FeSi) in the form of long, brittle intercepting platelets (or needles as they appear in the microstructure). These characteristics - brittleness and sharp plate-like morphology can act as stress concentrators and greatly affect to decrease the strength, ductility and dynamic fracture toughness of the castings (Seifeddine, 2007; Samuel et al., 2001; Shabestari, 2004; Ceschini et al., 2009).

The size and density of Fe-based intermetallic phases are increased with increasing % of Fe, also the dimensions of the defects and porosity of casting. Moreover, because they often form during solidification of the eutectic they may affect castability by interfering with interdendritic feeding and thus promote porosity (Tillová et al., 2011; Kuchariková et al., 2016; Samuel et al., 2014; Moustafa, 2009).

The present study is part of a larger research project VEGA which was conducted to study of secondary Al-Si cast alloys. The article describes the evaluation of Fe-rich phases in secondary AlSi7Mg0.3 cast alloys with amount 0.12 - 0.65 wt. % of Fe.

2 Materials and Methods

As an experimental material was used secondary (scrap-based - recycled) AlSi7Mg0.3 cast alloy with different percentage of iron (0.123; 0.454 and 0.655 wt. %). Chemical compositions of the experimental alloys composition was carried out by using arc spark spectroscopy and are given in Table 1. AlSi7Mg0.3 alloy has a good casting properties, very good machining, wear resistance and low thermal expansion. These Al-alloys have the widest application in mechanical engineering, cable car components, hydraulic and engine castings, mould constructions and etc. (Peter et. al., 2011; Tillová and Chalupová, 2009). Test bars (ø 20 mm with length 300 mm) were produced by process sand casting in foundry Zátor, Ltd. Czech Republic. Sand casting is the simplest and most widely used casting method. The melt was not modified or refined. We used casted bars without any heat treatment (in as cast state).

Table 1 Chemical composition of AlSi7Mg0.3 (wt. %) with different % of Fe

alloy	Si	Zn	Cu	**Fe**	Mg	Ti
A	7.028	0.036	0.013	**0.123**	0.354	0.123
B	7.340	0.020	0.021	**0.454**	0.302	0.118
C	7.315	0.028	0.030	**0.655**	0.292	0.118

In alloys A-C: Mn (0.009); Ni (0.002); Cr (0.002); Bi (0.0003); Sb (0.0007); Al (rest)

Metallographic samples (2 cm x 1.5 cm) were sectioned from the casted test bars and standard prepared for metallographic observations such as - wet ground on SiC papers, DP polished with 3 μm diamond past followed by Struers Op-S, etched by 0.5 % HF or H_2SO_4 (for helping the highlighting of Fe-intermetallic phases) (Tillová and Chalupová, 2009). Some samples were also deep-etched for 30 s in HCl solution in order to reveal the three-dimensional morphology of the silicon phase (Hurtalová et al., 2013). The specimen preparation procedure for deep-etching consists of dissolving the aluminium matrix in a reagent (36 % HCl) that will not attack the eutectic components or intermetallic phases. The residuals of the etching products should be removed by intensive rinsing in alcohol. The preliminary preparation of the specimen is not necessary, but removing the superficial deformed or contaminated layer can shorten the process.

The microstructure of experimental casts was studied using an optical microscope (Neophot 32) and scanning electron microscope (SEM) TESCAN VEGA LMU. To determine the chemical composition of the intermetallic phases was employed SEM with

EDX analyser BRUKER QUANTAX. Quantitative metallography was carried out on an Image Analyzer NIS Elements 4.2 to quantify porosity and Fe-phases. In order to minimize statistical errors in the determinations, 25 micrographs for each specimen were assessed; a relative error of less than 0.05 was sought.

Hardness was measured by Brinell hardness tester with a load of 250 kp (1 kp = 9.81 N), 5 mm diameter ball and a dwell time of 10 s (HBW 5/250/10). Five, at least, hardness measurements were taken for each specimen. The micro-hardness measurements of α-matrix and eutectic were performed using Vickers microhardness testing machine ZWICK/Roel ZHμ with the evaluation software ZWICK/Roel ZHμ/HD under a 2 g load for 10 s (HV 0.02) on metallographic samples. The evaluated HV 0.02 reflect average values of at least ten measurements on each structural parameter.

3 Results and Discussions

If the iron is present in Al-Si alloys, it is usually as the monoclinic/orthorhombic β-Al_5FeSi phase. This compound tends to form thin platelets (that appear as needles in section), which are very hard and brittle and have a relatively low bond strength with the matrix. Al_5FeSi needles are more unwanted, because adversely affect mechanical properties, especially ductility.

The deleterious effect of Al_5FeSi phase can be reduced by increasing the cooling rate, superheating the molten metal, or by the addition of a suitable "neutralizer" like Mn, Co, Cr, Ni, V, Mo and Be (Moustafa, 2009; Bolibruchová and Žihalová, 2013). The most common addition has been Mn. Excess Mn may reduce Al_5FeSi phase and promote formation Fe-rich phases $Al_{15}(FeMn)_3Si_2$ (known as alpha- or α-phase) in form "skeleton like" or in form "Chinese script" (Tillová and Chalupová, 2009; Tillová, et al., 2011; Borko et al., 2016; Taylor, 2004; 2012). If Mg is also present with Si, a pi-or π-phase $Al_5Fe_2Mg_8Si_6$ and script-like Mg_2Si can form.

The microstructure (Fig. 2, Fig. 3) of recycled AlSi7Mg0.3 cast alloys with different amount of iron consists of dendrites α-phase (white - 1), eutectic (mixture of α-matrix and spherical dark grey Si-phases - 2) and various types of intermetallic phases (3-5).

The α-matrix precipitates from the liquid as the primary phase in the form of dendrites and is nominally comprised of Al, Si and Mg. The different Fe- and Mg-rich intermetallic phases are concentrated mainly in the interdendritic spaces. These Fe- and Mg- intermetallic phases were identified by combination of the EDX results and light microscopy observation (morphology and different colors after etching).

It was found that increasing Fe-content from 0.123 to 0.655 wt. % has no significant effect on SDAS (Secondary Dendrite Arm Spacing) but the morphology of Al-Si eutectic became finer (Fig. 2).

The eutectic silicon appears as fibbers with a round cross-section (Fig. 2, a-c, on SEM). The 3-D form bars

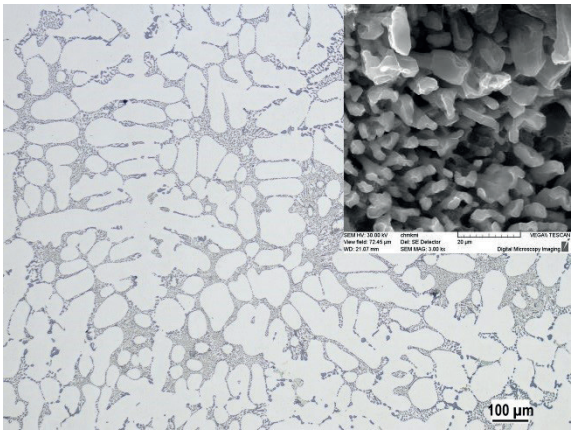

a) 0.123 % Fe

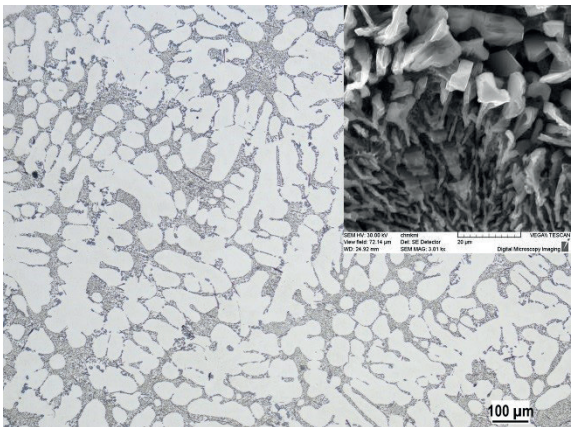

b) 0.454 % Fe

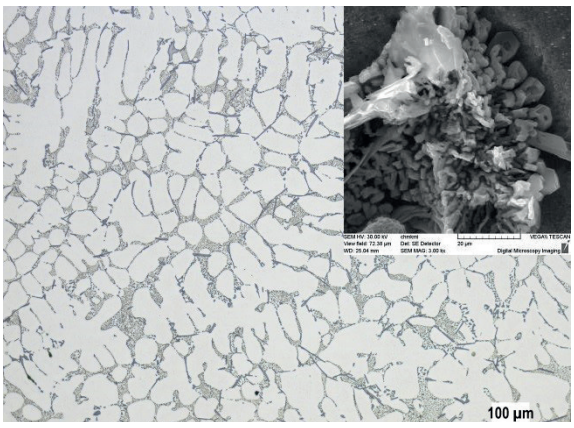

c) 0.655 % Fe

Fig. 2 Microstructure of experimental AlSi7Mg0.3 alloy, etch. 0.5 % HF; morphology of eutectic silicon, deep etch. HCl, SEM

corresponds with metallographic sections (Fig. 3), i.e. bunchy in the middle of the arrangement prevailing fine round bars and outwards, increased incidence of so called plate-like type with typical hexagonal shape can be observed as well, what is characteristic for the unmodified alloys.

Iron has a very low solid solubility in Al-alloy (maximum 0.05 % at equilibrium $Fe_{krit.}$ » 0.075 x (% Si) - 0.05), and most of iron form a wide variety of Fe-containing intermetallic depending on the alloy composition and its solidification conditions

(Tillová et al., 2011; Taylor, 2012; Rana et al., 2012). In accordance with Taylor, the two main types of Fe-rich intermetallic phases: Al_5FeSi (dark gray or black phase) and $Al_{15}(FeMn)_3Si_2$ (script-like light grey phase) were observed (Fig. 3). The ternary eutectic reaction (L → α + Si + Al_5FeSi) occurs at 576 °C and the maximum Fe-content to avoid the formation of primary β-Al_5FeSi is therefore rather low. Al_5FeSi phases precipitates already with content 0.123 % Fe in the interdendritic regions as platelets (needle like form when observed via microscope). Thickness of these platelets after deep etching was measured from 2 up to 5 μm (Fig. 4).

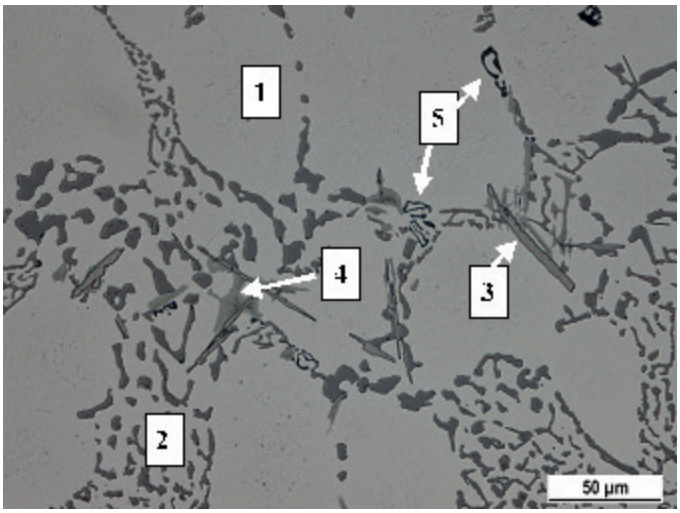

a) 0.123 % Fe

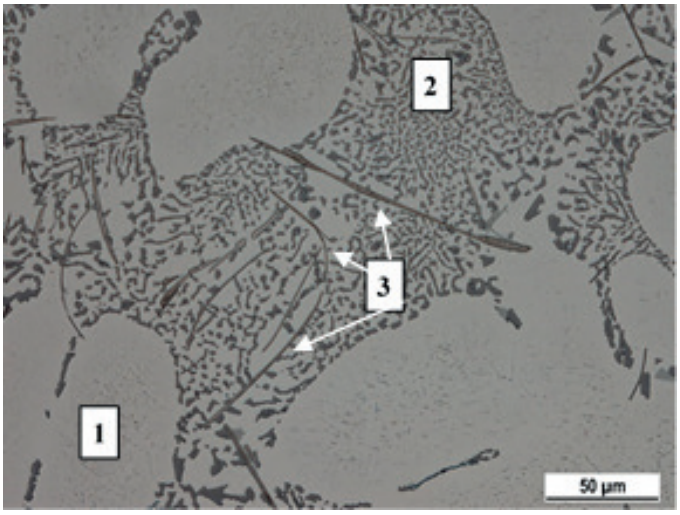

b) 0.454 % Fe

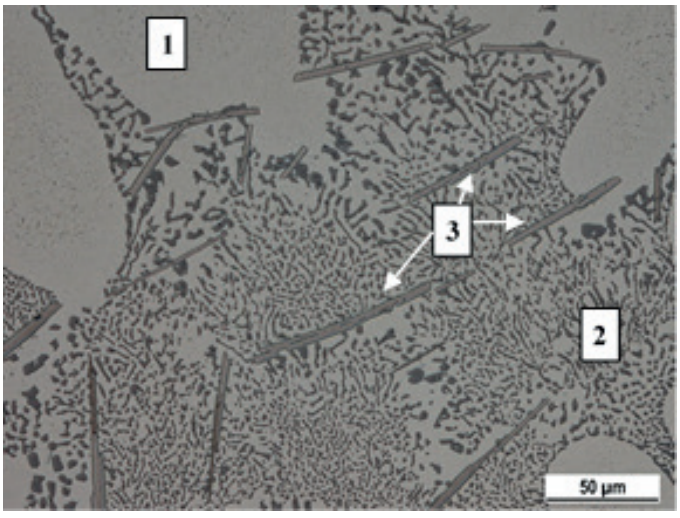

c) 0.655 % Fe

Fig. 3 Effect of iron on Fe-rich phases (1 - α-matrix; 2 - eutectic; 3 - Al_5FeSi; 4 - $Al_{15}(FeMg)_3Si_2$; 5 - Mg_2Si), etch. 0.5 % HF

Al_5FeSi platelets have been suggested as a possible nucleant for eutectic Si (Lu and Dahle, 2005). α-Al dendrites nucleate at the liquidus temperature, this is followed by the evolution of Fe-based Al_5FeSi phase at some temperature between the liquidus and eutectic temperature depending on the iron concentration. On further cooling to the eutectic temperature, eutectic silicon nucleates on these Al_5FeSi compounds ahead of the growing dendrites and grows as flakes into the liquid (Nafisi et al., 2008). This argument is based on the Al_5FeSi-detail observation after deep-etching (Fig. 4) that this phase was found to coexist and occur in close contact with eutectic Si.

Because in experimental material was not satisfied condition Fe : Mn = 2 : 1 (Taylor, 2012), Fe-rich phases in positive compact skeleton-like or in Chinese script form (phase $Al_{15}(FeMn)_3Si_2$) were observed very sporadically and predominantly in alloy A (0.123 % Fe). Dominant is needle-like Al_5FeSi phase. For all three alloys, the Mg_2Si phase with a black script-like morphology was also observed (Fig. 3a).

It is possible to observe that size and geometry of Fe-rich phases very depending on iron content. It was observed that in alloys A, B and C, the amount, size, and thickness of iron-based β-Al_5FeSi were found be increased (Fig. 3 and Fig. 5). Due to increasing iron content (from 0.123 to 0.655 wt. %), it was observed that average lengths of Al_5FeSi needles increased from 28.19 μm to 53.37 μm and needles became thicker (Fig. 5a - Fig. 5c).

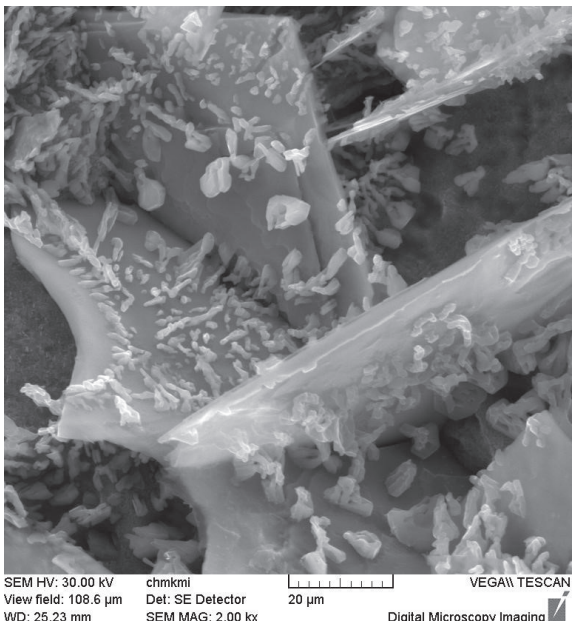

Fig. 4 Detail of morphology of plate-like Al_5FeSi phase with crystallization of silicon, deep etch. HCl, SEM

As indicated from Table 2, the maximal length of the needles is remarkably increased as the iron is increased (up to 90 %). Sporadically were found in alloy with 0.655 % of iron needles Al_5FeSi long more as 231 µm. It was also observed that as Fe content increased, α-$Al_{15}(FeMg)_3Si_2$ phases was transformed into Al_5FeSi. These results are in agreement with the works (Samuel et al., 2001; Moustafa, 2009). The total results (in average) of the quantitative evaluation of Fe-needles phases are shown in the Table 2.

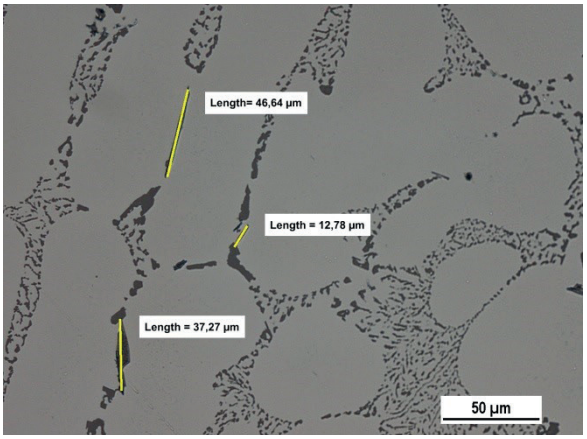

a) 0.123 % Fe

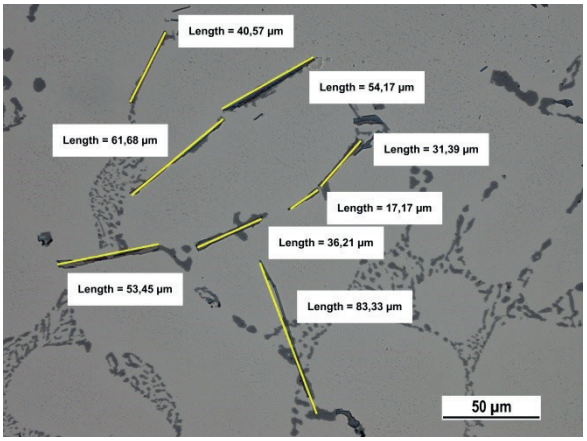

b) 0.454 % Fe

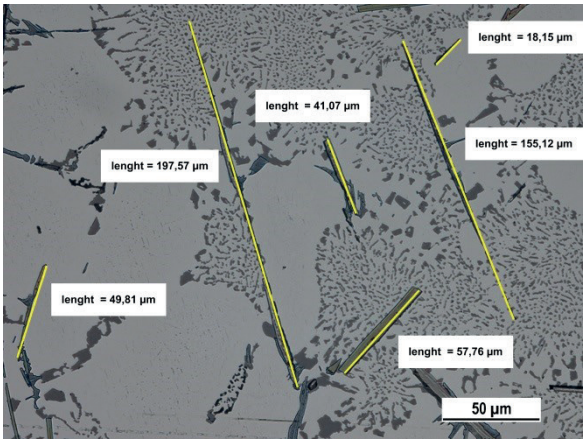

c) 0.655 % Fe

Fig. 5 Effect of iron on needle-like Al_5FeSi phase, etch. H_2SO_4

Table 2 Influence of iron on length of Fe-needle like phases

	wt. % of Fe		
	0.123	**0.454**	**0.655**
the average length of Fe-needles, µm	28.19	43.55	53.37
the maximum length of Fe-needles, µm	73.67	183.98	231.8

Porosity is one of the major factors that influence the mechanical properties. Fig. 6 illustrates the SEM macrographs of sectioned surfaces for different investigated alloys.

Porosity in experimental alloys A-C was observed directly proportional with Fe %. At a low iron content of iron (0.123 and 0.454 wt. %) in Fig. 6a, Fig. 6b sponge-like pores were observed first of all in the centre of the casting. Increasing Fe content from 0.123 to 0.655 wt. %, the casting shows a similar level of porosity (cca 1 - 1.5 % - Table 3), but distributed across a wider area (Fig. 6c) and locally there are large pores at the edge of the casting. Results of total porosity are in agreement with EN 1706 (www.raffmetal.com).

Table 3 Influence of iron on porosity

	wt. % of Fe		
	0.123	**0.454**	**0.655**
Shrinkage porosity, %	1	1.5	1.5
the average pore sizes, µm	20 878	16 031	18 788
the maximum pore sizes, µm	125 723	125 066	219 627

Differences in the average pore sizes between alloys A-C was observed minimal (Table 3). Due to increasing iron content (from 0.123 to 0.655 wt. %), it was observed that average pore sizes gently decreased from 20 878 µm to 18 788 µm, but with increasing iron content maximal pore size increased (from cca 125 723 µm to 219 627 µm). The increment reaches up to 74 %. Whereas the influence of Al_5FeSi needles on mechanical properties is negative, important are results of maximum pores sizes. Large iron rich needles which form early in the solidification process, tend to the formation of shrinkage porosity by blocking the interdendritic feeding channels.

Table 4 show the effect of Fe % on the hardness and microhardness. Brinell hardness of A-alloy (0.123 % Fe) was 49 HBW and is in agreement with EN 1706 (www.raffmetal.com). As can be seen, addition of Fe results in increase of Brinell hardness up to 4 and 8 %. The effect of iron on hardness can be described by the size and volume fraction of brittle and hard Al_5FeSi phase which are increased with iron content.

The results of microhardness test were supported by the microstructure images. Microhardness of α-matrix is with increasing iron content similar (cca 40 HV 0.02), but

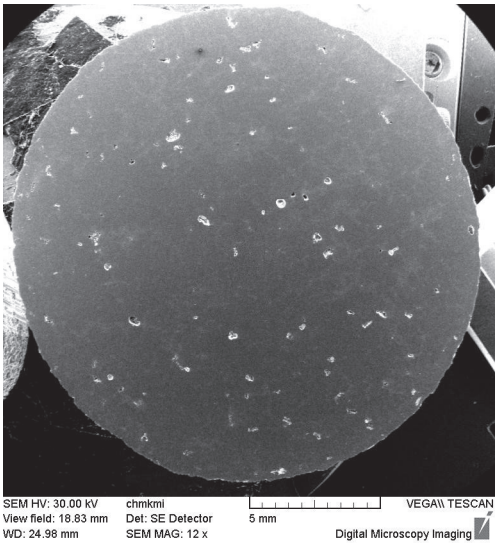

a) 0.123 % Fe

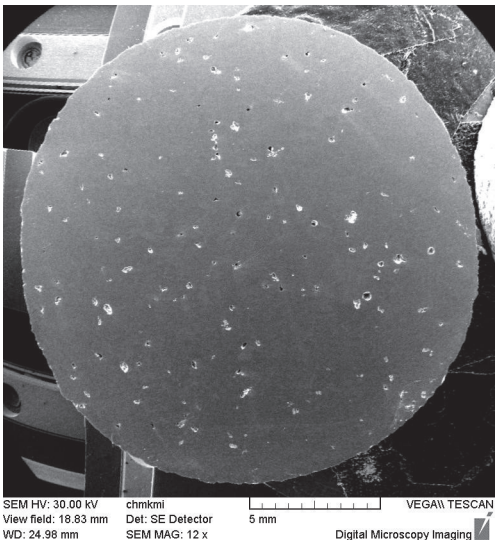

b) 0.454 % Fe

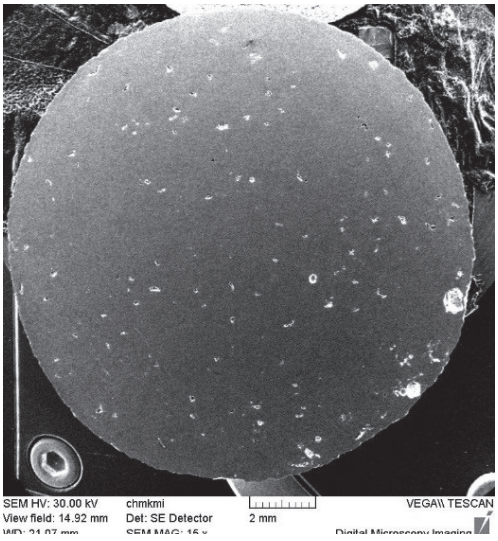

c) 0.655 % Fe

Fig. 6 SEM macrographs of the cross-section samples - effect of iron on porosity distribution, etch. 0.5 % HF

microhardnes of eutectic with increasing iron content increased from 48 HV 0.02 to 58 HV 0.02 (probably because of the higher number and thickening of the hard Al_5FeSi phases).

Table 4 Influence of iron on hardness and microhardness

	wt. % of Fe		
	0.123	**0.454**	**0.655**
HBS 5/250/10	49	51	53
HV 0.02 (in α-matrix)	40	39	40
HV 0.02 (in eutectic)	48	49	58

4 Conclusion

Addition of iron to secondary (recycled - scrap-based) AlSi7Mg0.3 cast alloy showing results:

- In experimental alloys were the two main types of Fe-rich intermetallic phases (needle-like Al_5FeSi and script-like $Al_{15}(FeMn)_3Si_2$) and script-like Mg_2Si phase identified.
- The volume fraction of Fe-rich intermetallic phases increases as the iron content increases. This increase has been found to be a result of size and the number of needle-like Al_5FeSi-phase.
- The increasing amount of iron has no effect on SDAS but the morphology of Al-Si eutectic became finer.
- A higher percentage of iron occurred to the progressive lengthening (on average) of a needle-like Fe-phase from 28.19 μm (alloy with 0.123 % Fe) to 53.37 μm (alloy with 0.655 % Fe). Sporadically were observed in alloy with 0.655 % of iron needles long more as 231 μm. $Al_{15}(FeMg)_3Si_2$ phases was transformed into Al_5FeSi.
- Due to increasing iron content (from 0.123 to 0.655 wt. %), it was observed that average pore sizes gently decreased, but maximal pore size increased (up to 74 %).
- We can to predict, that with the increasing amount of Fe decreasing the mechanical properties (first of all) ductility (through long β-Al_5FeSi intermetallic and high porosity).
- Addition of Fe results in increase of Brinell hardness; microhardness of α-matrix is similar and microhardnes of eutectic increased probably due to occurrence of the higher volume of Al_5FeSi phases.

Acknowledgement

This study has been supported by the Scientific Grant Agency of the Ministry of Education of the Slovak Republic VEGA 01/0533/15 and European Union project ITMS 26220220154.

References

Bolibruchová, D., Žihalová, M. (2013). Possibilities of iron elimination in aluminium alloys by vanadium. *Manufacturing Technology.* 13(3), pp. 289-296.

Borko, K., Tillová, E., Chalupová, M. (2016). The impact of Sr content on Fe - intermetallic phase's morphology changes in alloy AlSi10MgMn. *Manufacturing Technology.* 16(1), pp. 20-26.

Ceschini, L., Boromei, I., Morri, A., Seifeddine, S., Svensson, I. L. (2009). Microstructure, tensile and fatigue properties of the Al-10% Si-2% Cu alloy with different Fe and Mn content cast under controlled conditions. *Journal of Materials Processing Technology.* 209(15–16), pp. 5669–5679. https://doi.org/10.1016/j.jmatprotec.2009.05.030

European Aluminium Association. [Online] Available from: http://www.aluplanet.com/eng/eaa.asp [Accessed: 1st January 2017]

Hurtalová, L., Tillová, E., Chalupová, M. (2013). Effect of heat treatment on fracture surfaces in recycled aluminium cast alloy. *Periodica Polytechnica Transportation Engineering.* 41(2), pp. 117-122. https://doi.org/10.3311/PPtr.7111

Kuchariková, L., Tillová, E., Bokůvka, O. (2016). Recycling and Properties of Recycled Aluminium Alloys Used in the Transportation Industry. *Transport Problems.* 11(2), pp. 117-122. https://doi.org/10.20858/tp.2016.11.2.11

Lu, L., Dahle, A. K. (2005). Iron-Rich Intermetallic Phases and Their Role in Casting Defect Formation in Hypoeutectic Al-Si Alloys. *Metallurgical and Materials Transactions A.* 36(13), pp. 819-835. https://doi.org/10.1007/s11661-005-1012-4

McMillan, C. A., Skerlos, S. J., Keoleian, G. A. (2012). Evaluation of the Metals Industry's Position on Recycling and its Implications for Environmental Emissions. *Journal of Industrial Ecology.* 16(3), pp. 324–333. https://doi.org/10.1111/j.1530-9290.2012.00483.x

Moustafa, M. A. (2009). Effect of iron content on the formation of β-Al_5FeSi and porosity in Al–Si eutectic alloys. *Journal of Materials Processing Technology.* 209(1), pp. 605–610. https://doi.org/10.1016/j.jmatprotec.2008.02.073

Nafisi, S., Ghomashchi, R., Vali, H. (2008). Eutectic nucleation in hypoeutectic Al-Si alloys. *Materials Characterization.* 59(10), pp. 1466–1473. https://doi.org/10.1016/j.matchar.2008.01.014

Peter, I., Varga, B., Rosso, M. (2011). Dimensional stability analysis in Al-Si alloys. *Metalurgia International.* 16, pp. 5-9.

Rana, R. S., Purohit, R., Das, S. (2012). Reviews on the Influences of Alloying elements on the Microstructure and Mechanical Properties of Aluminum Alloys and Aluminum Alloy Composites. *International Journal of Scientific and Research Publications.* 2(6), pp.1-7.

Samuel, A. M., Samuel, F. H., Villeneuve, C., Doty, H. W., Valtiera, S. (2001). Effect of trace elements on β-Al_5FeSi characteristics, porosity and tensile properties of Al–Si–Cu (319) cast alloys. *International Journal of Cast Metals Research.* 14(2), pp. 97–120. https://doi.org/10.1080/13640461.2001.11819429

Samuel, E., Samuel, A. M., Doty, H. W., Valtierra, S., Samuel, F. H. (2014). Intermetallic phases in Al-Si based cast alloys: new perspective. *International Journal of Cast Metals Research.* 27(2), pp. 107-114. https://doi.org/10.1179/1743133613Y.0000000083

Schlesinger, M. E. (2014). *Aluminum Recycling.* 2nd ed. CRC Press, Boca Raton, Florida, USA.

Seifeddine, S. (2007). The influence of Fe on the microstructure and mechanical properties of cast Al-Si alloys. *Literature review - Vilmer project.* Jönköping University, Sweden.

Shabestari, S. G. (2004). The effect of iron and manganese on the formation of intermetallic compounds in aluminum-silicon alloys. *Materials Science and Engineering: A.* 383(2), pp. 289–298. https://doi.org/10.1016/j.msea.2004.06.022

Taylor, J. A. (2004). The effect of iron in Al-Si casting alloys. In: Casting Concepts. 35th Australian Foundry Institute National Conference. Adelaide, South Australia, Oct. 31 - Nov. 3, 2004. pp. 148-157.

Taylor, J. A. (2012). Iron-Containing Intermetallic Phases in Al-Si Based Casting Alloys. *Procedia Materials Science.* 1, pp. 19-33. https://doi.org/10.1016/j.mspro.2012.06.004

Tillová, E., Chalupová, M., Hurtalová, L., Ďuriníková, E. (2011). Quality control of microstructure in recycled Al-Si cast alloys. *Manufacturing Technology.* 11, pp. 70-76.

Tillová, E., Chalupová, M. (2009). Štruktúrna analýza. (Structural analysis.) EDIS ZU, Žilina (in Slovak).

www.raffmetal.com [Accessed 1st January 2017]